

# LANS: A Layout-Aware Neural Solver for Plane Geometry Problem

Ming-Liang Zhang<sup>1,2\*</sup>, Zhong-Zhi Li<sup>1,2\*</sup>, Fei Yin<sup>1,2</sup>, Cheng-Lin Liu<sup>1,2†</sup>

<sup>1</sup>MAIS, Institute of Automation, Chinese Academy of Sciences, Beijing, 100190, China

<sup>2</sup>School of Artificial Intelligence, University of Chinese Academy of Sciences, Beijing, 100049, China  
 {zhangmingliang2018, lizhongzhi2022}@ia.ac.cn, {fyin, liucl}@nlpr.ia.ac.cn

## Abstract

Geometry problem solving (GPS) is a challenging mathematical reasoning task requiring multi-modal understanding, fusion and reasoning. Existing neural solvers take GPS as a vision-language task but be short in the representation of geometry diagrams which carry rich and complex layout information. In this paper, we propose a layout-aware neural solver named LANS, integrated with two new modules: multimodal layout-aware pre-trained language model (MLA-PLM) and layout-aware fusion attention (LA-FA). MLA-PLM adopts structural and semantic pre-training (SSP) to implement global relationship modeling, and point matching pre-training (PMP) to achieve alignment between visual points and textual points. LA-FA employs a layout-aware attention mask to realize point-guided cross-modal fusion for further boosting layout awareness of LANS. Extensive experiments on datasets Geometry3K and PGPS9K validate the effectiveness of the layout-aware modules and superior problem solving performance of our LANS solver, over existing symbolic solvers and neural solvers. The code will make public available soon.

## 1. Introduction

Automatic geometry problem solving (GPS) is a long-standing and challenging research topic in both computer vision (CV) and natural language processing (NLP) communities [2, 7, 29]. One geometry problem consists of a geometry diagram and a textual problem that describe in different modal forms and complement each other. GPS necessitates comprehensive mathematical reasoning and multi-modal understanding, making it a pivotal testbed for evaluating the high-level multimodal reasoning ability of artificial intelligence. Past research works of GPS were mainly focused on *symbolic solvers* [20, 28, 29], which are criticized in respect of complex rules and poor adaptability.

\*Equal contribution.

†Corresponding author.

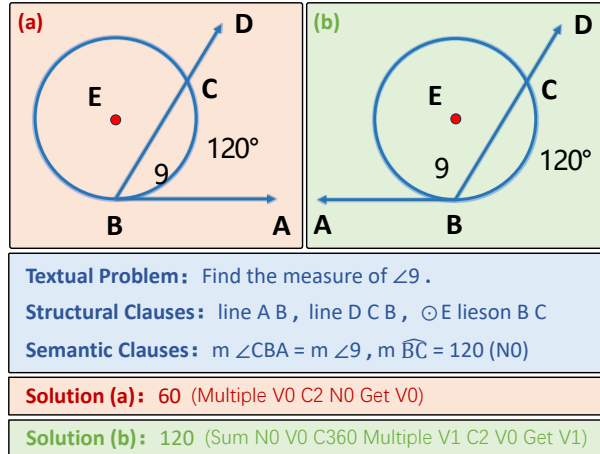


Figure 1. Examples of plane geometry problem. The geometry diagrams (a) and (b) share the same textual problem, structural clauses and semantic clauses but have different solutions, where structural clauses and semantic clauses are parsed from diagrams. Layout information plays crucial roles in this situation.

ity. With the development of deep learning, *neural solvers* [4, 5, 36], treating GPS as a special vision-language reasoning task, have attracted dominant attention recently. The core of neural solvers for GPS lies in the multimodal understanding and fusion.

In GPS, the understanding and fusion of geometry diagram is one of key challenges but usually overlooked by recent GPS works. As shown in Figure 1, the geometry diagram often has a complex layout in which the geometric primitives (point, line and circle) and the non-geometric primitives (text and symbol) are related to each other spatially, structurally and semantically. The structural clause “line B C D” describes a structural relationship that points “B”, “C” and “D” lie on one line in order. The semantic clause “ $m \widehat{BC} = 120$ ” illustrates a semantic relationship for the degree of arc “ $\widehat{BC}$ ” and text “120°”. “ $\angle CBA$ ” in Figure 1 (a) and (b) need the spatial relationship to determine whether it is acute or obtuse. To sum up, the geometry diagram carries rich layout content and provides crucial roles

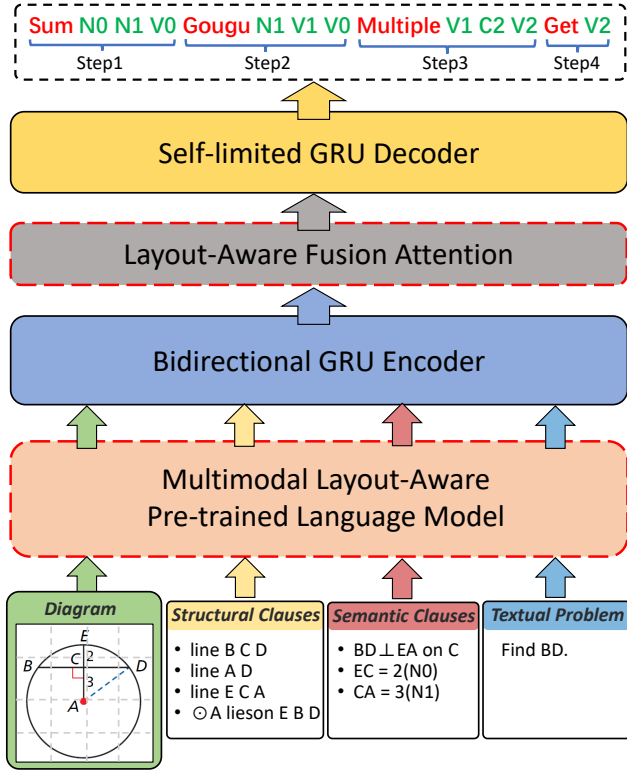


Figure 2. Overview of LANS model. The red dotted boxes are our newly proposed modules in comparison to PGPSSNet[36].

to aid problem solving.

Existing neural solvers have adopted different diagram representation schemes, such as *feature maps* [3, 4, 25], *image patches* [5, 25] and *textual clauses* [20, 36]. Due to the structural richness of geometry diagram, the feature maps and image patches, commonly used in nature scene image representation [1, 9, 34], are not capable of extracting fine-grained structural and semantic contents in diagrams. Textual clauses are more suitable for expressing fine-grained and multi-level structural information in geometry diagram, they lose significant spatial information during the conversion process of diagram parsing [24]. For example, the textual clauses cannot distinguish the geometry diagram (a) and (b) displayed in Figure 1 because of the loss of position information. To enhance the representation of geometry diagram, auxiliary tasks have been proposed, such as jigsaw location prediction [4], geometry elements prediction [4], masked image modeling [25] and character alignment [25]. However, these methods are coarse-grained and shallow, do not grasp spatial layout sufficiently.

Considering the under-representation of geometry diagram, as shown in Figure 2, we propose a layout-aware neural solver called LANS. LANS inputs the diagram image, the textual clauses parsed from diagram and the textual problem, and outputs the explainable solution program to

solve geometry problem. Above all, two new modules, multimodal layout-aware pre-trained language model (MLA-PLM) and layout-aware fusion attention (LA-FA), are proposed to endow LANS with layout awareness. MLA-PLM adopts two pre-training strategies during the pre-training stage. The first is structural and semantic pre-training (SSP) based on masked language modeling (MLM) only for text. By the language modeling for textual clauses with local correlation, LANS acquires the ability of global relationship cognition. The second is point matching pre-training (PMP) based on contrastive learning modeling (CLM) across image and text. PMP realizes the alignment of visual points and textual points via matching image patches and points inside image patches, thus embeds spatial information into textual clauses. Compared with the common and direct strategy of fine-grained position embedding [16, 32, 33], PMP is more effective for pre-training on small-scale dataset as is the case in GPS. In fact, the spatial position at image patch level is sufficient to understand the layout of plane geometry diagram, also consistent with geometric cognition of human. During the training stage, LA-FA with the layout-aware attention mask is employed in LANS to fuse diagram and text via point positions. Different from the general global visible self-attention [31], LA-FA attends intra-modal tokens unconditionally but attends cross-modal tokens only if textual points are located in image patches. The LA-FA module further enhances the layout awareness in cross-modal fusion.

The contributions of this work are summarized in four folds: (1) We propose a layout-aware neural solver LANS for GPS, which can represent and fuse geometry diagram effectively. (2) We introduce the MLA-PLM module with two pre-training strategies SSP and PMP, realizing global relationship modeling and cross-modal alignment of point primitives. (3) We design the LA-FA module, equipping with layout-aware attention mask directed by point positions, to further strengthen the layout awareness of LANS. (4) Our LANS outperforms existing symbolic solvers and neural solvers significantly on Geometry3K and PGPSSNet datasets [36].

## 2. Related Work

### 2.1. Multimodal Reasoning

Multimodal reasoning combines multimodal information to carry out reasoning, often in the form of questions and answers, e.g., visual question answering [1, 15], document visual question answering [30, 32] and table question answering [23, 37]. To achieve correct multi-modal reasoning, it is first necessary to understand and integrate multimodal content, and then applies domain knowledge to solve problem logically. The knowledge types investigated in multimodal reasoning include semantics [21, 32], common

sense [13, 32], spatial location [14, 22], numerical quantity [14, 23], color [13, 21] and so on. GPS is a special type of multimodal reasoning that examines geometric spatial structure cognition and mathematical logical reasoning, and also requires the application of geometric theorem knowledge, making it highly challenging.

## 2.2. Geometry Problem Solving

Existing works of GPS can be classified into two categories: symbolic solvers and neural solvers. The symbolic solvers [20, 26, 28, 29] parse the diagram and textual problem into a unified formal language firstly, and then perform symbolic reasoning by path search and condition matching based on the geometric theorem knowledge. However, symbolic solvers are carefully designed with complex rules and hard to extend. The neural solvers treat GPS as a visual question answering task and design a special interpretable program to represent the problem solving process. NGS [4] and Geformer [5] used auxiliary self-supervised tasks such as location prediction, elements prediction and knowledge classification to boost cross-modal semantic representation. PGPSNet [36] expressed diagram with textual clauses and fuses multi-modal information through structural and semantic pre-training, data augmentation and self-limited decoding. SCA-GPS [25] tried to align character in text and diagram and enhances the diagram understanding through multi-label classification and masked image modeling pre-training. Although existing neural solvers have achieved impressive performance, they are still coarse-grained at the modal understanding and fusion, especially for geometry diagrams with complex layouts. In this paper, we propose a layout-aware neural solver to improve the understanding and fusion of geometry diagram and therefore promote problem solving.

## 2.3. Multimodal Pre-training

Multimodal pre-training realizes alignment and understanding between different modalities by a series of designed auxiliary tasks, and then applies to the specific downstream tasks. Common strategies involve image-text contrastive learning [27], image-text matching [15], image-grounded text generation [6] and masked object classification [16]. With a large amount of pre-training data, these strategies exhibit good performance in multimodal tasks for natural images. However, their alignment methods are coarse-grained and violent and do not fit for complex multi-level and fine-grained tasks. Most relevant to our work is the research on document analysis [18]. Existing advanced document pre-training methods [32, 33] incorporate textual and visual blocks with fine-grained position embeddings, and adopt masked visual-language modeling and text-image alignment to pretrain document layout, whereas they still do not apply to GPS due to the specificity of geometry objects

and small-scale of GPS datasets. Our LANS proposes targeted and data-efficient pre-training methods to implement geometry layout awareness.

## 3. Model

Before presenting the neural solver model, we first describe the formal definition of GPS task here. Given a geometry problem  $P$  including a geometry diagram  $D$  and a textual problem  $T_{prob}$ , the goal is to solve problem applying geometric knowledge and obtain the solution steps  $S$ , formulated as  $P = \{D, T_{prob}\} \Rightarrow S$ . The solution steps are verified in the form of fill-in-the-blank, multiple choice or logic reason.

### 3.1. Overall Framework

To fully understand and represent the geometry diagram, we propose a layout-aware neural solver called LANS as displayed in Figure 2. First, the diagram is parsed into the textual clauses using the geometry diagram parser PGDPNet [35], where the structural clauses  $T_{stru}$  describe the connection relations among geometric primitives and the semantic clauses  $T_{sem}$  depict the semantic relations between non-geometric primitives and geometric primitives [36]. Besides, the visual information of diagram image is represented as patches. Therefore, the input of LANS could be further expressed as  $\{D = \{d_i\}_{i=1}^{N_D}, T = \{T_{stru}, T_{sem}, T_{prob}\} = \{t_j\}_{j=1}^{N_T}\}$  after token concatenation, where  $N_D$  is the diagram patch number and  $N_T$  is the text token number. Then, these modal tokens are fed into the multimodal layout-aware pre-trained language model (MLA-PLM) to realize cross-modal layout understanding, and input into the bidirectional GRU encoder to perform fusion encoding. Next, the mixed encoding context  $H = \{h_i\}_{i=1}^{N_D+N_T}$  leverages the layout-aware fusion attention (LA-FA) to further boost diagram layout awareness. Finally, the enhanced context is decoded by the self-limited GRU decoder and generates the sequential solution program  $S$  in the manner of autoregressive.

It is worth noting that LANS adopts the same bidirectional GRU encoder and self-limited GRU decoder as the PGPSNet solver [36], instead of the transformer encoder and decoder [31] used commonly. This is because without large-scale pre-training, the performance of transformer-based models is usually worse than GRU-based models especially for small-scale datasets. The modules of MLA-PLM and LA-FA are our major contributions of this work and will be introduced in detail in the following.

### 3.2. Multimodal Layout-Aware Pre-training

Geometry problems are often solved by humans by depicting the geometric structure in visual form no matter whether it has the geometry diagram or not. Previous neural geomet-

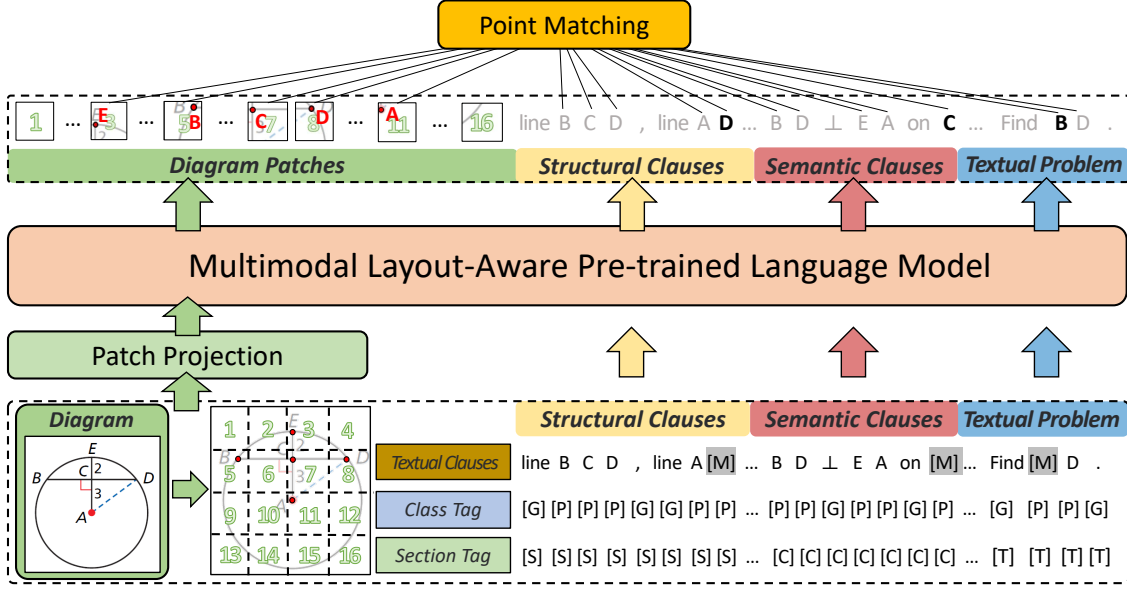


Figure 3. Pipeline of multimodal layout-aware pre-training. The geometry problem is the same as that in Figure 2. [M] denotes mask tokens. Class tags and section tags are the same as [36].

ric solvers, such as the NGS [4], PGPSSNet [36] and SCA-GPS [25], do not utilize the diagram layout adequately, thus resulting in unsatisfactory performance of GPS. In this paper, we propose the multimodal layout-aware pre-trained language model (MLA-PLM), with two pre-training strategies: structural and semantic pre-training (SSP) and point matching pre-training (PMP) illustrated in Figure 3, to boost the diagram layout-aware ability during the pre-training stage.

While the textual clauses well express the fine-grained and multi-level content of geometry diagram, they are lacking in overall structural and semantic cognition. Therefore, we propose the SSP based on the masked language modeling (MLM) [8] to endow the global layout cognition. Besides, we propose the PMP based on contrastive learning modeling (CLM) to achieve cross-modal alignment between visual points (one type of geometric primitives in diagram) and textual tokens of the points. Concretely, inputs of MLA-PLM include the diagram patch embeddings  $e_i^D$  and textual token embeddings  $e_j^T$ , where  $e_i^D$  is obtained via patch projection and patch-level positional encoding, and  $e_j^T$  fuses not only positional encoding but also embedding of class tag and section tag following [36], formulated as:

$$\begin{aligned} e_i^D &= \text{PatchProj}(d_i) + \text{PosEmb}(i), \quad 1 \leq i \leq N_D \\ e_j^T &= \text{TokenEmb}(t_j) + \text{PosEmb}(j) + \text{ClassEmb}(t_j), \quad (1) \\ &\quad + \text{SectEmb}(t_j), \quad 1 \leq j \leq N_T \end{aligned}$$

where  $\text{PosEmb}(*)$  is the sequential position encoding of sequences instead of spatial position of diagram layout. The

concatenated  $e_i^D$  and  $e_j^T$  are modeled by MLA-PLM and then output  $e_i^D$  and  $e_j^T$ . For SSP in MLA-PLM, we mask 30% of text tokens  $t_j$  with mask token [M] following [6] but keep tags unchanged. MLA-PLM is trained to recover the masked text in a unified text generation manner, and the training loss denotes as  $L_{SSP}$ . For PMP, we match image patches and points inside image patches with the cosine contrastive loss [10, 12] as following:

$$L_{PMP} = -\frac{1}{|\mathcal{P}|} \sum_{j \in \mathcal{P}} \log \frac{\exp(\cos(e_j^T, e_+^D)/\tau)}{\sum_{i=1}^{N_D} \exp(\cos(e_j^T, e_i^D)/\tau)}, \quad (2)$$

where  $\mathcal{P} = \{j \mid \text{Class}(t_j) = [\text{P}], 1 \leq j \leq N_T\}$  is the index list of text tokens corresponding to points,  $e_+^D$  is the embedding of the diagram patch that the point  $t_j$  is located in, and  $\tau$  is the temperature coefficient that empirically set as 0.1. Combining SSP and PMP, our pre-training process is a multi-task learning with the mixed training loss  $L_{all} = L_{SSP} + L_{PMP}$ .

By combining two pre-training strategies SSP and PMP, the solver strengthens the cognition of complex geometry layout. In SSP, the modeling of local relationships leads to the global relationship understanding, for example, we can infer that the mask token in the semantic clause “BD  $\perp$  EA on [M]” is “C” according to structural clauses “line B C D” and “line E C A”. Via PMP, the textual points become aware of layout position from positional encoded image patches by alignment. We do not adopt the simple and direct way of fine-grained 2D position embedding such as in LayoutLM [32, 33]. This is because existing GPS datasets do not sup-

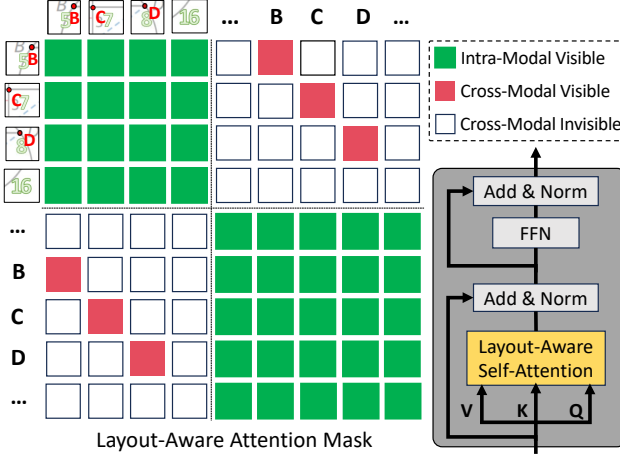


Figure 4. Schematic of Layout-Aware Fusion Attention.

port large-scale layout understanding pre-training. And it is also akin to human geometric cognition in that accurate positioning is not required to understand geometry layout.

### 3.3. Layout-Aware Fusion Attention

Although LANS has already acquired a certain level of layout understanding through the pre-training strategies above, this ability can fade to some extent during downstream training because of the different training target of GPS. To compensate the loss of layout awareness in the GPS training phase, we propose the layout-aware fusion attention (LA-FA) to enhance the intra-modal and cross-modal token fusion. LA-FA is located between the bidirectional GRU encoder and self-limited GRU decoder.

As shown in Figure 4, LA-FA module is similar to the transformer encoder block [31] which also contains layer normalization, feed forward layer and residual connection except the layout-aware self-attention. Our layout-aware self-attention uses the carefully designed layout-aware attention mask which allows visibility to all intra-modality tokens, but restricts cross-modality visibility only if the textual point is inside the image patch in the visual space. Specifically, we construct the mask matrix  $M_{i,j}$  ( $1 \leq i, j \leq N_D + N_T$ ), which consists of value 0 as invisible and value 1 as visible:

$$M_{i,j} = \begin{cases} 1, & (i, j) \in VV \\ 1, & (i, j) \in TT \\ 1, & (i, j) \in VT \text{ & } \text{Pos}(t_j) \in \text{Reg}(d_i) \\ 0, & \text{otherwise} \end{cases}, \quad (3)$$

where  $VV = \{(i, j) \mid 1 \leq i, j \leq N_D\}$  is the mask region of visual intra-modality,  $TT = \{(i, j) \mid N_D + 1 \leq i, j \leq N_D + N_T\}$  is the mask region of textual intra-modality,  $VT = \{(i, j) \mid 1 \leq i, j \leq N_D + N_T\} - VV - TT$  is the mask region of

cross-modality,  $\text{Pos}(t_j)$  denotes the visual position of point token  $t_j$  and  $\text{Reg}(d_i)$  refers to the visual region of image patch  $d_i$ . Moreover, our layout-aware self-attention LASA could be computed by:

$$\text{LASA}(Q, K, V, M) = \text{softmax} \left( \frac{QK^T}{\sqrt{m_k}} \cdot M \right) V \quad (4)$$

where  $Q, K, V$  are query matrix, key matrix and value matrix all transformed from encoding context  $H$ , and  $m_k$  is the dimension of key vector.

In summary, in the process of cross-modal fusion, LA-FA leverages the point position to guide the attention between diagram and text, strengthening the understanding of diagram layout. For mitigating the optimization burden, we only use one LA-FA block, while adding more blocks does not bring extra improvement according to our experiments.

## 4. Experiments

### 4.1. Setup

#### 4.1.1 Implementation details.

**Model architecture.** The patch projection module for diagram chooses the CNN architecture, selecting a light-weight ResNet10 [11] to extract feature map before meshing. Feeding with diagram images resized as  $256 \times 256$ , the patch projection module maps diagram into  $8 \times 8 = 64$  image patches. In default, we employ a 6-layer, 8-head, 256-input and 1024-hidden dimensional transformer [31] as the architecture of MLA-PLA, and a multi-head attention with the same head number and feature dimension for LA-FA. The bidirectional GRU encoder and self-limited GRU decoder in LANS are adopted the same architecture as PGPSNet [36]. Besides, a dropout layer with value 0.2 is added behind the patch projection module to prevent overfitting during the training stage.

**Optimization method.** We choose the AdamW optimizer [19] with the weight decay  $1 \times 10^{-2}$  and the step decline schedule with the decay rate of 0.5, and the training batch size is set as 128. During the pre-training phase, the learning rate is initialized to  $5 \times 10^{-4}$  and the learning rate decay is applied at 1,000, 1,800, 2,400 and 3,000 epochs with a total of 3,500 epochs. During the training stage, all modules of LANS train together with initial learning rate as  $1e^{-4}$  for language model MLA-PLM and  $1e^{-3}$  for other modules, decaying at 160, 280, 360, 440 and 500 epochs uniformly with a total 520 epochs.

**Data augmentation.** As to geometry diagram, we scale image to 256 on the longest side and place it in the center of  $256 \times 256$  blank screen. The diagram is flipped randomly and changes the point positions accordingly. For text, following the work [36], we apply four augmentation strategies: token replacement, connection rotation, representation transposition and clauses shuffle. These augmentation

Table 1. Performance comparison among state-of-the-art GPS solvers. \* denotes results re-produced with the open source code. & denotes methods re-implemented by us.

Method	Geometry3K			PGPS9K		
	Completion	Choice	Top-3	Completion	Choice	Top-3
Human Expert [20]	-	90.9	-	-	-	-
Baseline (Neural Solver) [20]	-	35.9	-	-	-	-
InterGPS (Predict)* [20]	44.6	56.9	-	-	-	-
InterGPS (Diagram GT)* [20]	64.2	71.7	-	59.8	68.0	-
InterGPS (All GT)* [20]	69.0	75.9	-	-	-	-
GeoDRL (Predict) [26]	-	68.4	-	-	-	-
NGS& [4]	35.3	58.8	62.0	34.1	46.1	60.9
Geoformer& [5]	36.8	59.3	62.5	35.6	47.3	62.3
SCA-GPS [25]	-	76.7	-	-	-	-
PGPSNet [36]	65.0	77.9	80.7	62.7	70.4	79.5
LANS	<b>72.1</b>	<b>82.3</b>	<b>82.8</b>	<b>66.7</b>	<b>74.0</b>	<b>82.2</b>

strategies not only improve the diversity of geometry problems, but also provide geometric solvers with basic geometric representation knowledge.

#### 4.1.2 Datasets and Metrics

We evaluate the performance of proposed LANS on two plane geometry problem datasets: Geometry3K [20] and PGPS9K [36]. They are all collected from American geometry textbooks across 6-12 grades covering 30 problem types, where Geometry3K has 8,433 training samples and 589 test samples, and PGPS9K is evenly divided into training set 8,022 and test set 1,000 according to the problem type. Moreover, they all have fine-grained diagram annotation and interpretable solution program. The textual clauses and point positions used in this paper are converted from the diagram annotation. The solution program consists of several solving steps, each step consists of an operator and associated operands, where operator corresponds to a geometric theorem and operands are arranged according to the theorem formula. The paired program executor based on Python calculates numerical results of solution programs. The MLA-PLA module of LANS is pretrained from scratch on PGPS9K dataset that masks solution programs, because of the shortage of geometric corpus and the great distribution gap in contrast with natural corpus.

Similar to PGPSNet [36], we use three evaluation metrics to assess the numerical performance of our LANS, namely *Completion*, *Choice* and *Top-3*. In the *Completion*, the neural solver selects the first executable solution program as the *Completion* result. The *Choice* is defined as choosing the correct option from four candidates but selecting one randomly if answer is not in. In the *Top-3*, the solution is considered correct if it is among the top three confidence solutions. We set the *Completion* as evaluation

metric for ablation study in section 4.3 by default.

#### 4.2. Comparison with State-of-the-art Models

We compare with state-of-the-art models including symbolic solvers and neural solvers to show superior problem solving performance of LANS as illustrated in Table 1.

As to symbolic solvers, InterGPS [20] solved geometry problems by searching and matching with unified formal language. According to the input source of formal language, InterGPS presents with three types of results, e.g., “Predict” means that all formal language are predicted by its parsers, “Diagram GT” denotes that formal clauses of diagram use ground truth, and “All GT” indicates that formal clauses of diagram and textual problem are all ground truth. GeoDRL [26] improved the search strategy of InterGPS with logical graph deduction and deep reinforcement learning. Experimental results show that our LANS outperforms symbolic solvers on all datasets and in all evaluation metrics. Even compared with InterGPS (All GT) that uses annotated formal clauses designed carefully, LANS gains a 3.1% improvement in *Completion* and a 6.4% improvement in *Choice* on Geometry3K.

As to neural solvers, NGS [4] and Geoformer [5] relied primarily on the textual problem to solve problems. Even through re-implementing them with the textual clauses parsed from diagram and the same augmentation strategies, performance gaps between these two solvers and our LANS are still significant, 32.6% and 31.1% lower in *Completion* on PGPS9K, respectively. SCA-GPS [25] shows similar performance as InterGPS (All GT) because diagram understanding methods, character alignments and masked image modeling, are coarse-grained and ineffective. PGPSNet [36] employed textual clauses to model diagram layout but lost lots of visual information. Our LANS is enhanced at

modal alignment and fusion for better layout awareness, and surpasses PGPSNet by 7.1% and 4.0% in Completion on Geometry3K and PGPS9K.

In addition, our LANS is a light-weight model with similar parameter count as PGPSNet, but much smaller than other solvers. The improvements in Top-3 are less than in Completion because most of correct solutions are concentrated among high confident candidates. Besides, there remains a certain performance gap between LANS and human expert, still has much room for improvement.

### 4.3. Ablation Study

#### 4.3.1 Effect of Modules

To examine the effect of our proposed modules in LANS, we conducted ablation experiments on the Geometry3K dataset, taking PGPSNet solver [36] who owns SS-PLM module but without LA-FA module as the baseline. Experimental results presented in Table 2 illustrate that MLA-PLM module with multimodal pre-training is superior to SS-PLM module with only text-modal pre-training and obtain a 5.4% improvement. LA-FA module further boosts GPS via multi-modal feature fusion in the training phase and achieves a 72.1% accuracy, over baseline 7.1%.

Table 2. Ablation study of modules on Geometry3K.

Module	Accuracy
Baseline	65.0
+ MLA-PLM	70.4 (+5.4)
+ MLA-PLM + LA-FA	<b>72.1</b> (+7.1)

Table 3. Ablation study of patch projection.

Projection Type	Geometry3K	PGPS9K
None	64.2	61.3
Linear	69.4	65.5
CNN	<b>72.1</b>	<b>66.7</b>

#### 4.3.2 Impact of Patch Projection

To validate the impact of patch projection schemes, in Table 3, we tested three types of patch projection module: None, linear layer and CNN model. None refers to not using patch projection module and also not inputting image patches. In our experiments, we find that redundant placeholder in None do harm to GPS due to additional meaningless optimizations. The linear-based patch projection maps image grids linearly and produces corresponding image patches, which is also commonly adopted in recent transformer architectures [15, 17]. However, this module is not fit to ge-

ometry diagram because it may damage the geometric structure. CNN-based patch projection first extracts global features and then mesh feature maps. That module could better understand the overall layout, bringing with higher solving performance and more stable training, and it is also set as the default patch projection module.

#### 4.3.3 Influence of Image Patches

To assess the influence of image patches, we adopted four configurations of patch numbers:  $1 \times 1$ ,  $4 \times 4$ ,  $8 \times 8$  and  $16 \times 16$ . In Table 4, we observe that LANS benefits from fine-grained partitions of diagram, based on the comparison of row 1 with row 2, 3, 4. However, according to the comparison of row 3 with row 4, problem solving performance declines if diagram is over-segmented. The possible explanation is that redundant and blank image grids, which are generated from patch partition, interference model attention while increase the burden of model computation. Therefore, considering overall performance and speed, we choose the  $8 \times 8$  configuration as our model setup.

Table 4. Ablation study of image patch number.

Image Patch Number	Geometry3K	PGPS9K
$1 \times 1$	65.0	62.7
$4 \times 4$	70.5	<b>66.8</b>
$8 \times 8$	<b>72.1</b>	66.7
$16 \times 16$	69.1	65.4

#### 4.3.4 Role of Pre-training Strategies

To validate the role of pre-training strategies within MLA-PLM, we did ablation experiments on both SSP and PMP pre-training strategies. Ablation experiments involved two processes: first pre-training with various strategies and then fine-tuning on Geometry3K. Table 5 verifies that SSP and PMP pre-training strategies all improve GPS, where SSP promotes the global relationship recognition and PMP aligns visual points and textual points. The comparison between row 2, row 3 and row 4 demonstrates that the combination of SSP and PMP realizes complex layout understanding synthetically, thus promotes problem solving together.

Table 5. Ablation study of pre-training strategies on Geometry3K.

Pre-training Strategy	Accuracy
None	38.2
+ SSP	55.4 (+17.2)
+ PMP	66.9 (+28.7)
+ SSP + PMP	<b>72.1</b> (+33.9)

**(a)**

**Problem:**  
Find  $z$ .  
**Choices:**  
A 132.0; B 138.0; C 142.0; D 148.0  
**Answer:** C

**Structural Clauses**  
• line A I K  
• line B H G  
• line C E F  
• line J I H E D

**Semantic Clauses**  
•  $CF // BG // AK$   
•  $m \angle HIK = 2y+8$  (N0)  
•  $m \angle JIK = 142$  (N1)  
•  $m \angle IHG = 4x+6$  (N2)  
•  $m \angle DEC = z$  (N3)

**NGS:** Equal V0 N2 Sum V0 N0 C180 Get z  
**PGPSNet:** Sum N1 N3 C180 Get z  
**LANS & GT:** Equal N1 N3 Get z

**(b)**

**Problem:**  
Find the area of the figure. Perimeter = 90 (N0) centimeters.  
**Choices:**  
A 387.1; B 540.0; C 584.6; D 21044.4  
**Answer:** C

**Structural Clauses**  
• line K L  
• line M L  
• line H J

**Semantic Clauses**  
•  $GH = GM = HJ$   
•  $LM = KL = JK$

**NGS:** Multiple V0 C5 N0 RNgon\_B\_Area C5 V0 V1 Get V1  
**PGPSNet:** Multiple V0 C6 N0 RNgon\_B\_Area C5 V0 V1 Get V1  
**LANS & GT:** Multiple V0 C6 N0 RNgon\_B\_Area C6 V0 V1 Get V1

**(c)**

**Problem:**  
Find the measure of  $\angle 9$ .  
**Choices:**  
A 60.0; B 120.0; C 240.0; D 300.0  
**Answer:** C

**Structural Clauses**  
• line A B  
• line D C B  
•  $\odot E$  lies on B C

**Semantic Clauses**  
•  $m \angle CBA = m \angle 9$   
•  $m \angle BDC = 120$  (N0)

**NGS:** Sum NO C90 V0 Sum N1 V0 V1 Get V1  
**PGPSNet:** Multiple V0 C2 NO Get V0  
**LANS & GT:** Sum NO V0 C360 Multiple V1 C2 V0 Get V1

**(d)**

**Problem:**  
Assume the segments that appear to be tangent are tangent. Find the length of AC.  
**Choices:**  
A 18.0; B 23.0; C 41.0; D 46.0  
**Answer:** D

**Structural Clauses**  
• line A B C  
• line A D E  
•  $\odot H$  lies on C G E  
•  $\odot F$  lies on B D G

**Semantic Clauses**  
•  $AB = 23$  (N0)  
•  $DA = x$  (N1)  
•  $CB = x-5$  (N2)

**NGS:** Equal NO N1 Equal V0 N2 Get V0  
**PGPSNet:** Equal NO N2 Sum NO N2 V0 Equal V0 V1 Get V1  
**LANS:** Equal NO N1 Sum NO N2 V0 Equal V0 V1 Get V1  
**GT:** Equal NO N1 Sum NO N2 V0 Get V0

Figure 5. Case analysis on PGP9K. Solving above problems requires layout awareness of geometry diagram. (a), (b) and (c) are the problems LANS answered correctly, (d) is the problem LANS answered incorrectly.

#### 4.3.5 Role of Attention Mask

To validate the role of attention mask within the LA-FA module, we compare with three types of attention masks: w/o LA-FA, vanilla attention mask [31], and layout-aware attention mask. Compared with the vanilla attention mask with global visibility, layout-aware attention mask guided by point positions promotes modal fusion and strengthens diagram understanding. The results in Table 6 also indicate that compared with the vanilla attention mask, the role of our layout-aware attention mask is significant.

Table 6. Ablation study of attention mask on Geometry3K.

Mask Type	Accuracy
w/o LA-FA	70.4
w Vanilla Attention Mask [31]	70.6
w Layout-Aware Attention Mask	<b>72.1</b>

#### 4.4. Case Analysis

We also conducted case analysis to discuss the strengths and weaknesses of solvers. Figure 5 displays four plane geometry problems (a)-(d) involving various geometric layout, and they rely on good layout awareness to solve them. In case (a), the positional relationship between C and F determines the relationship between the  $\angle JIK$  and  $\angle DEC$  whether are corresponding angles or alternate angles. The solution results illustrate that LANS distinguishes the corresponding

angles correctly while other solvers are misguided. In case (b), the perception of polygon edge number is the key to solving this problem. Contrary to LANS, NGS and PGP9K cannot count edge number correctly through diagram or textual clauses, resulting in a wrong solution. Case (c) is the same problem as shown in Figure 1 in which textual clauses cannot identify diagram uniquely. In contrast with PGP9K, LANS can judge the orientation and type of  $\angle ABC$  and gets the right solution. Case (d) is a complex layout scenario that none of solvers can be solved correctly. In conclusion, case analyses above fully indicate that LANS promotes GPS with enhanced layout awareness.

## 5. Conclusion

We propose a layout-aware neural solver LANS to understand and fuse complex layouts of plane geometry diagrams, thus promoting geometric logic reasoning. Benefiting from the multimodal layout-aware pre-training, consisting of the SSP and PMP, LANS is endowed with abilities of global relationship cognition and cross-modal point alignment. In the training, thanks to the layout-aware fusion attention, LANS further improves cross-modal fusion directed by point positions. The experimental results also demonstrate superiority of our LANS solver enhanced with layout awareness. However, our LANS is still limited to point primitives to carry out layout understanding. In the future, we will try to align higher-level geometric primitives to obtain better layout understanding and modal fusion.

## References

[1] Peter Anderson, Xiaodong He, Chris Buehler, Damien Teney, Mark Johnson, Stephen Gould, and Lei Zhang. Bottom-up and top-down attention for image captioning and visual question answering. In *CVPR*, 2018. 2

[2] Daniel G. Bobrow. Natural language input for a computer problem solving system. *Semantic Information Processing*, 1968. 1

[3] Jie Cao and Jing Xiao. An augmented benchmark dataset for geometric question answering through dual parallel text encoding. *COLING*, 29, 2022. 2

[4] Jiaqi Chen, Jianheng Tang, Jinghui Qin, Xiaodan Liang, Lingbo Liu, Eric P. Xing, and Liang Lin. GeoQA: A geometric question answering benchmark towards multimodal numerical reasoning. In *Findings of ACL*, 2021. 1, 2, 3, 4, 6

[5] Jiaqi Chen, Tong Li, Jinghui Qin, Pan Lu, Liang Lin, Chongyu Chen, and Xiaodan Liang. UniGeo: Unifying geometry logical reasoning via reformulating mathematical expression. In *EMNLP*, 2022. 1, 2, 3, 6

[6] Jaemin Cho, Jie Lei, Hao Tan, and Mohit Bansal. Unifying vision-and-language tasks via text generation. In *ICML*, 2021. 3, 4

[7] Shang Ching Chou, Xiao Shan Gao, and Jing Zhong Zhang. Automated generation of readable proofs with geometric invariants: II. Theorem proving with full-Angles. *Journal of Automated Reasoning*, 17(3), 1996. 1

[8] Jacob Devlin, Ming-Wei Chang, Kenton Lee, and Kristina Toutanova. BERT: Pre-training of deep bidirectional transformers for language understanding. In *NAACL*, 2019. 4

[9] Yang Ding, Jing Yu, Bang Liu, Yue Hu, Mingxin Cui, and Qi Wu. Mukea: Multimodal knowledge extraction and accumulation for knowledge-based visual question answering. In *CVPR*, 2022. 2

[10] Jean-Bastien Grill, Florian Strub, Florent Altché, Corentin Tallec, Pierre Richemond, Elena Buchatskaya, Carl Doersch, Bernardo Avila Pires, Zhaohan Guo, Mohammad Gheshlaghi Azar, et al. Bootstrap your own latent-a new approach to self-supervised learning. In *NeurIPS*, 2020. 4

[11] Kaiming He, Xiangyu Zhang, Shaoqing Ren, and Jian Sun. Deep residual learning for image recognition. In *CVPR*, 2016. 5

[12] Kaiming He, Haoqi Fan, Yuxin Wu, Saining Xie, and Ross Girshick. Momentum contrast for unsupervised visual representation learning. In *CVPR*, 2020. 4

[13] Drew A Hudson and Christopher D Manning. Gqa: A new dataset for real-world visual reasoning and compositional question answering. In *CVPR*, 2019. 3

[14] Justin Johnson, Li Fei-Fei, Bharath Hariharan, C. Lawrence Zitnick, Laurens Van Der Maaten, and Ross Girshick. Clevr: A diagnostic dataset for compositional language and elementary visual reasoning. In *CVPR*, 2017. 3

[15] Wonjae Kim, Bokyung Son, and Ildoo Kim. Vilt: Vision-and-language transformer without convolution or region supervision. In *ICML*, 2021. 2, 3, 7

[16] Gen Li, Nan Duan, Yuejian Fang, Ming Gong, and Dixin Jiang. Unicoder-vl: A universal encoder for vision and language by cross-modal pre-training. In *AAAI*, 2020. 2, 3

[17] Junnan Li, Dongxu Li, Caiming Xiong, and Steven Hoi. BLIP: Bootstrapping language-image pre-training for unified vision-language understanding and generation. In *ICML*, 2022. 7

[18] Cheng-Lin Liu, Lianwen Jin, Xiang Bai, Xiaohui Li, and Fei Yin. Frontiers of intelligent document analysis and recognition: review and prospects. *Journal of Image and Graphics*, 28(08):2223–2252, 2023. 3

[19] Ilya Loshchilov and Frank Hutter. Decoupled weight decay regularization. In *ICLR*, 2017. 5

[20] Pan Lu, Ran Gong, Shibiao Jiang, Liang Qiu, Siyuan Huang, Xiaodan Liang, and Song Chun Zhu. Inter-GPS: Interpretable geometry problem solving with formal language and symbolic reasoning. In *ACL*, 2021. 1, 2, 3, 6

[21] Pan Lu, Liang Qiu, Jiaqi Chen, Tony Xia, Yizhou Zhao, Wei Zhang, Zhou Yu, Xiaodan Liang, and Song-Chun Zhu. IconQA: A new benchmark for abstract diagram understanding and visual language reasoning. In *NeurIPS, Track on Datasets and Benchmarks*, 2021. 2, 3

[22] Pan Lu, Swaroop Mishra, Tanglin Xia, Liang Qiu, Kai-Wei Chang, Song-Chun Zhu, Oyvind Tafjord, Peter Clark, and Ashwin Kalyan. Learn to explain: Multimodal reasoning via thought chains for science question answering. In *NeurIPS*, 2022. 3

[23] Pan Lu, Liang Qiu, Kai-Wei Chang, Ying Nian Wu, Song-Chun Zhu, Tanmay Rajpurohit, Peter Clark, and Ashwin Kalyan. Dynamic prompt learning via policy gradient for semi-structured mathematical reasoning. In *ICLR*, 2023. 2, 3

[24] Pan Lu, Liang Qiu, Wenhao Yu, Sean Welleck, and Kai-Wei Chang. A survey of deep learning for mathematical reasoning. In *ACL*, 2023. 2

[25] Maizhen Ning, Qiu-Feng Wang, Kaizhu Huang, and Xiaowei Huang. A symbolic characters aware model for solving geometry problems. In *ACM MM*, 2023. 2, 3, 4, 6

[26] Shuai Peng, Di Fu, Yijun Liang, Liangcai Gao, and Zhi Tang. GeoDRL: A self-learning framework for geometry problem solving using reinforcement learning in deductive reasoning. In *Findings of ACL*, 2023. 3, 6

[27] Alec Radford, Jong Wook Kim, Chris Hallacy, Aditya Ramesh, Gabriel Goh, Sandhini Agarwal, Girish Sastry, Amanda Askell, Pamela Mishkin, Jack Clark, et al. Learning transferable visual models from natural language supervision. In *ICML*, 2021. 3

[28] Mirinmaya Sachan and Eric Xing. Learning to solve geometry problems from natural language demonstrations in textbooks. In *SEM*, 2017. 1, 3

[29] Minjoon Seo, Hannaneh Hajishirzi, Ali Farhadi, Oren Etzioni, and Clint Malcolm. Solving geometry problems: Combining text and diagram interpretation. In *EMNLP*, 2015. 1, 3

[30] Rubèn Tito, Dimosthenis Karatzas, and Ernest Valveny. Document collection visual question answering. In *ICDAR*, 2021. 2

[31] Ashish Vaswani, Noam Shazeer, Niki Parmar, Jakob Uszkoreit, Llion Jones, Aidan N. Gomez, Łukasz Kaiser, and Illia Polosukhin. Attention is all you need. In *NeurIPS*, 2017. 2, 3, 5, 8

- [32] Yiheng Xu, Minghao Li, Lei Cui, Shaohan Huang, Furu Wei, and Ming Zhou. LayoutLM: Pre-training of text and layout for document image understanding. In *SIGKDD*, 2020. [2](#), [3](#), [4](#)
- [33] Yang Xu, Yiheng Xu, Tengchao Lv, Lei Cui, Furu Wei, Guoxin Wang, Yijuan Lu, Dinei Florencio, Cha Zhang, Wanxiang Che, Min Zhang, and Lidong Zhou. Layoutlmv2: Multi-modal pre-training for visually-rich document understanding. In *ACL*, 2021. [2](#), [3](#), [4](#)
- [34] Zhou Yu, Jun Yu, Yuhao Cui, Dacheng Tao, and Qi Tian. Deep modular co-attention networks for visual question answering. In *CVPR*, 2019. [2](#)
- [35] Ming-Liang Zhang, Fei Yin, Yihan Hao, and Cheng-Lin Liu. Plane geometry diagram parsing. In *IJCAI*, 2022. [3](#)
- [36] Ming-Liang Zhang, Fei Yin, and Cheng-Lin Liu. A multi-modal neural geometric solver with textual clauses parsed from diagram. In *IJCAI*, 2023. [1](#), [2](#), [3](#), [4](#), [5](#), [6](#), [7](#)
- [37] Fengbin Zhu, Wenqiang Lei, Youcheng Huang, Chao Wang, Shuo Zhang, Jiancheng Lv, Fuli Feng, and Tat-Seng Chua. TAT-QA: A question answering benchmark on a hybrid of tabular and textual content in finance. In *ACL*, 2021. [2](#)